International Journal of Automotive Technology, Vol. 7, No. 5, pp. 637−644 (2006)

1229−9138/2006/029−15

DEVELOPMENT OF A NEW MISFIRE DETECTION SYSTEM USING NEURAL NETWORK

M. LEE[1)], M. YOON[1)], M. SUNWOO[2)*], S. PARK[3)] and K. LEE[3)]

[1)]Graduate School of Automotive Engineering, Hanyang University, Seoul 133-791, Korea
[2)]Department of Automotive Engineering, Hanyang University, Seoul 133-791, Korea
[3)]Hyundai Motor Company, 772-1 Jangdeok-dong, Hwaseong-si, Gyeonggi 445-706, Korea

(Received 25 October 2005; Revised 3 March 2006)

ABSTRACT−The detection of engine misfire events is one of major concerns in engine control due to its negative effect on air pollution and engine performance. In this paper, a misfire detection system based on crankshaft angular speed fluctuation is developed. Synthetic variable method is adopted for the preprocessing of crankshaft angular speed. This method successfully estimates the work output of each cylinder by finding the effect of combustion energy on the crankshaft rotational speed or acceleration after virtually removing the effect of the internal inertia forces from the measured crankshaft speed signals. The detection system is developed using neural network with the revised synthetic angular acceleration as input which is derived from the preprocessing. Mathematical simulation is carried out for developing and verifying the misfire detection system. Finally, the reliability of the developed system is validated through an experiment.

KEY WORDS : Misfire, Synthetic variables, Neural network

NOMENCLATURE

$J(\theta)$: moment of inertia, a function of crankshaft angular position [kgm^2]
$\bar{J}$: constant moment of inertia [kgm^2]
J_c : moment of inertia of connecting rod about rod mass center [kgm^2]
$J_i(\theta)$: moment of inertia of connecting rod and piston about the crankshaft axis [kgm^2]
J_s : moment of inertia of crankshaft and flywheel about the crankshaft axis [kgm^2]
K : polytropic index [−]
L : center-to-center length of connecting rod [m]
L_2 : distance from connecting rod mass center to crank end center [m]
m_c : mass of connecting rod and bearings [kg]
m_p : mass of piston and wrist pin assembly [kg]
n : cylinder number [−]
P : cylinder pressure [Pa]
R : crank radius [m]
$T_{friction/pumping}$: friction and pumping torque [kgm]
$T_{external}$: external torque [kgm]
t : time [s]
V : cylinder volume [m^3]
ε : compression ratio [−]
θ : angular displacement of crankshaft [rad]
$\dot{\theta}$: angular velocity [rad/s]
$\ddot{\theta}$: angular acceleration [rad/s^2]
τ : stroke number [−]

SUBSCIPTS

ce : compression and expansion
comb : combustion
ic : inlet close
rev : removing comression/expansion work
syn : synthetic

**Corresponding author.* e-mail: msunwoo@hanyang.ac.kr

1. INTRODUCTION

Misfire is a condition in which there is little combustion due to ignition failure, lack of fuel, or insufficient compression, etc. Misfires are grouped into two types: random misfire and continuous misfire. Random misfires occur intermittently due to engine operation and road condition. Continuous misfires are repeating misfires caused by abnormal operation of the ignition plug, injector, intake/exhaust valve malfunction, etc. Misfires create partial burn or unburned exhaust gas. Thus, they are major sources of air pollution, and they damage catalysts mounted on all gasoline engine vehicles. Moreover, repetitive misfires increase engine vibration and noise which damage the stiffness of vehicle body. Therefore, the detection of engine misfire events is a major concern in automotive engineering due to its relation to air pollution and engine performance.

In recent years, air pollution has become worse due to rising vehicle exhaust gas emissions. As a result new stringent regulations have been invoked such as OBD-II and EURO-III in America and Europe. Therefore, the development of misfire detection system is now one of the major research areas in the automotive industry. Misfire detection systems use crankshaft speed fluctuations (Förster *et al.*, 1990; Wu *et al.*, 1998; Moro *et al.*, 1998; Nareid *et al.*, 2004; Mahieu *et al.*, 2000), exhaust gas pressure (Ceccarani *et al.*, 1998; Willimowski *et al.*, 2000), cylinder chamber ionic current (VanDyne *et al.*, 2000) and structure-borne sound (Villarion *et al.*, 2004) for detecting misfire events. The two major considerations in the design of a misfire detection system are the cost and the detection rate of the misfire detection method. In this regard, the best detection method is crankshaft speed detection unlike the other three methods. Crankshaft speed based detection does not require any additional sensors which reduces the cost. However, its detection rate is not as high as the other method, but high enough to provide the necessary level of performance.

In this paper, a misfire detection system using crankshaft angular speed fluctuation is developed. When misfires occur, insufficient torque is generated due to reduced combustion in the cylinder. The generated torque from combustions can be used for detecting misfire. However, direct measurement of the generated torque is impossible. Thus an estimation method for engine torque using crankshaft speed is generally employed. This method has some advantages in terms of cost and performance. Also it is better suited for mass production since it is less complex than the other techniques. However it has some difficulties for detecting individual cylinder misfire particularly during low load, high speed operations.

The misfire detection procedure for this research is shown in Figure 1. The first stage is acquiring the engine crankshaft speed. The second is preprocessing and feature extraction in order to transform the raw speed data into the proper form. The last stage is pattern recognition for detecting misfire events using a neural network. Mathematical simulation is carried for developing and verifying the misfire detection system. Then the reliability of the developed system is validated through an experimental data.

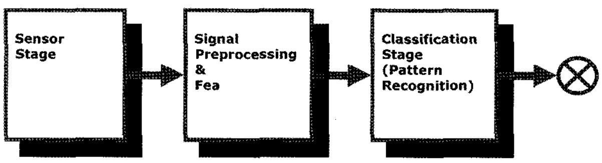

Figure 1. Misfire detection procedure.

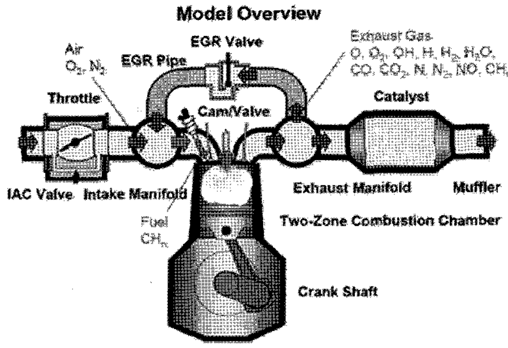

Figure 2. Engine++ model overview.

2. ENGINE MODEL FOR MISFIRE DETECTION SYSTEM

Development time and cost for designing control or diagnosis system can be reduced by math-model based simulations (Yoon *et al.*, 2005). However, the mathematical model must be accurate enough to represent the real plant. A very precise model, such as a cylinder-by-cylinder combustion model, is needed for developing a misfire detection system based on crankshaft angular velocity fluctuation.

2.1. Selection of Engine Model

A preprocessing and detecting algorithm can be easily developed by math-model based simulation without any experiment. In order to detect misfires with crankshaft speed fluctuations, torque generation resulted by combustions for each cylinder must be needed, so that the crankshaft speed fluctuation appears in simulation results. There are some widespread commercial engine models such as Engine++ by SimuQuest, EngineSim by SimCar, and GT-Power by Gamma technology. Among these three engine models, the Engine++ is appropriate for developing misfire detection system because the Engine++ has cylinder-by-cylinder combustion models, and is fast and accurate enough for designing misfire detection system.

2.2. Features of Engine++

Engine++ is a MATLAB Simulink block based engine model. Some or the general features of this model are described in Figure 2. With Engine++ mathematical models for each part such as throttle, intake manifold, combustion chamber, exhaust manifold can be customized according to the user's purposes. It is a very reliable model because it is a zero-dimensional model. It is also physics based model derived from the mass and energy conservation. Moreover, the better performances and reliabilities are obtained by separating the exhaust gases into 12 different partial gases.

3. PREPROCESSING FOR MISFIRE DETECTION

The misfire detection system performs data acquisition, preprocessing and feature extraction, and classification (Figure 1). In this chapter, a preprocessing method using synthetic variables (Moskwa *et al.*, 2000) is explained in terms of detection target selection and preprocessing.

3.1. Preprocessing with Synthetic Variables

A crankshaft angular speed fluctuation based misfire detection method has the advantage of utilizing crankshaft speed sensors, such as an optical encoder or a magnetic pickup which are widely available, relatively robust and inexpensive. This enables to a non-intrusive, reliable and practical strategy of engine diagnostics with the methods of pattern recognition or model-based diagnostics. However, with this method it is difficult to determine combustion quality in small and medium size SI and CI engines because internal rotational inertia force originating from the reciprocating mechanism is varies greatly with respect to the engine speed. In order to overcome these difficulties, synthetic variables for crankshaft speed are utilized. This approach is to successfully estimate the work output of each cylinder by finding the affects of combustion energy on the crankshaft rotational speed or acceleration after electrically removing the effects of the internal inertia forces from the measured crankshaft speed signals. Additionally, this approach can be used for an engine control because of their simplicity, linearity and consistency.

3.1.1. Crankshaft rotational dynamics

Crankshaft rotational dynamics can be modeled in many ways depending on the intended use of the model. Some models assume that the crankshaft, connecting rod and piston assemblies in the engine can be considered as having a constant rotational polar inertia when viewed from the perspective of crankshaft rotation. This is often used in control when requiring simplified and linear models, and is a reasonable assumption for a well-balanced engine with multi-cylinders. If the crankshaft with this assumption is chosen as a free body and Newton's second law is applied, the dynamic equation can be expressed as follows.

$$\bar{J}\cdot\ddot{\theta}=\sum_{i=1}^{n}P_i\cdot\frac{\partial V_i}{\partial\theta}+\sum T_{friction/pump}+\sum T_{external} \tag{1}$$

The indicated torque from each cylinder, load torque from the drivetrain and any ancillary devices, and friction/pumping torque are applied to the crankshaft causing its acceleration and deceleration.

But the polar moment of inertia is not constant in an actual engine and it is related to a few factors such as mass, geometry, configuration, and crankangle. In the version of the model used in this paper, the engine rotational dynamics utilize a rigid crankshaft model with fully nonlinear rotational dynamics. All of the crank-angle-varying inertial effects that result from the slider-crank mechanism of each cylinder (e.g., the crankshaft/con-rod/piston kinematics) are included in the dynamic equation because the dynamic effects from these linkages increase dramatically at high engine speeds. Its governing equation derived from Lagrange's methodsneglecting the gravity force, is given as:

$$\begin{aligned}&J(\theta)\cdot\ddot{\theta}+\frac{1}{2}\cdot\frac{\partial J(\theta)}{\partial\theta}\cdot\dot{\theta}^2\\&=\sum_{i=1}^{n}P_i\cdot\frac{\partial V_i}{\partial\theta}+\sum T_{friction/pumping}+\sum T_{external}\end{aligned} \tag{2}$$

In equation (2), the inertia depends on the engine's physical parameters and is a function of crankshaft angular position. For an individual cylinder, the polar moment axis is given as follows (Shiao *et al.*, 1994).

$$\begin{aligned}J_i(\theta)&=J_c\frac{R^2\cos^2\theta}{L^2-R^2\sin^2\theta}+m_cR^2\cos^2\theta\left(1-\frac{L_2}{L}\right)^2\\&+m_cR^2\sin^2\theta\left(1+\frac{L_2R\cos\theta}{L\sqrt{L^2-R^2\sin^2\theta}}\right)^2\\&+m_pR^2\sin^2\theta\left(1+\frac{R\cos\theta}{\sqrt{L^2-R^2\sin^2\theta}}\right)^2\end{aligned} \tag{3}$$

Its derivative with respect to θ is given.

$$\begin{aligned}\frac{\partial J_i(\theta)}{\partial\theta}&=\left[m_p+\frac{L_2}{L}\left(2-\frac{L_2}{L}\right)m_c-\frac{J_c\left(L^2-R^2\right)}{L^2-R^2\sin^2\theta}\right]\sin 2\theta\\&+\frac{Lm_p+L_2m_c}{L\sqrt[3]{L^2-R^2\sin^2\theta}}R^3\cdot\\&\left[2L^2\sin\theta\left(3\cos^2-1\right)-2R^2\sin^3\theta\cos^2\theta\right]\\&+\frac{L^2m_p+L_2^2m_c}{L^2\left(L^2-R^2\sin^2\theta\right)}R^4\sin 2\theta\cdot\\&\left[\cos 2\theta+\frac{R^2\sin^2\theta}{4\left(L^2-R^2\sin^2\theta\right)}\right]\end{aligned} \tag{4}$$

For a typical engine with even firing orders, the varying inertia and its derivatives of the slider-crank mechanism can be expressed as follows:

$$J(\theta)=J_s+\sum_{i=1}^{n}J_i\left(\theta-\frac{720}{n}(i-1)\frac{\tau}{4}\right) \tag{5}$$

$$\frac{\partial J(\theta)}{\partial\theta}=\sum_{i=1}^{n}\frac{\partial J_i\left(\theta-180(i-1)\cdot\tau/n\right)}{\partial\theta} \tag{6}$$

3.1.2. Synthetic variables

By comparing equation (1) and (2), one can see that the right-hand sides are identical for any working engine. Therefore, the left-hand sides equal each other as shown in equation (7). $\bar{J}$ is independent of the crankangle because the constant inertia engine model takes only the polar moment of inertia into consideration and treats it as a constant value. This means that the constant inertia engine model not only ignores the engine inertia variations, but also fails to accommodate the effects of the velocity related inertia torque. A methodology, therefore, has been put forward. The real measured engine speed can be combined with the nonlinear rotating dynamics to remove the varying inertia effects and generate a linear "synthetic" acceleration as shown in the following equations.

$$\bar{J}\ddot{\theta}_{syn}=J(\theta)\ddot{\theta}+\frac{1}{2}\frac{\partial J(\theta)}{\partial\theta}\dot{\theta}^2 \tag{7}$$

This equation can then be rearranged and integrated to produce an expression that can generate another linear "synthetic" engine speed.

$$\ddot{\theta}_{syn}=\frac{J(\theta)}{\bar{J}}\ddot{\theta}+\frac{1}{2\bar{J}}\frac{\partial J(\theta)}{\partial\theta}\dot{\theta}^2 \tag{8}$$

$$\dot{\theta}_{syn}=\frac{J(\theta)}{\bar{J}}\dot{\theta}-\frac{1}{2\bar{J}}\int\frac{\partial J(\theta)}{\partial\theta}\dot{\theta}^2dt \tag{9}$$

The benefits of using these "synthetic" variables are several. Firstly, the actual nonlinear engine rotational dynamics can be treated as linear when using the "synthetic" acceleration and velocity. This will greatly simplify the control and diagnostics tasks. Secondly, the waveform of the "synthetic" variables do not change as the mean engine speed changes, therefore the speed dependency is completely eliminated which can mean a large reduction in the size of the diagnostic strategy code. Another benefit is that the "synthetic" acceleration is directly proportional to summation of applied torques. If the external load torque and friction/pumping torque are known, the torque from combustion can then be clearly identified.

3.1.3. Modifications for compression/expansion work

As presented in equations (1) and (2), the rotation of the crankshaft is the result of indicated torque from combustion pressure and other external torques applied on the shaft. Therefore, the net working gas torque causes the crankshaft to accelerate or decelerate when the engine is running without load. The working gas pressure is composed of the pressure in compression/expansion and those that increase due to combustion during this process. If the periodically changed compression/expansion work can be removed from the working gas torque, only the torque from combustion will remain and its effects will probably be more apparent and not masked by compression and expansion work.

Based on the distribution and combination law, the working gas torque can be rearranged as follows.

$$\sum_{i=1}^{n}P_i\frac{\partial V_i}{\partial\theta}=\sum_{i=1}^{n}P_{ce,i}\frac{\partial V_i}{\partial\theta}+\sum_{i=1}^{n}P_{comb,i}\frac{\partial V_i}{\partial\theta} \tag{10}$$

$P_{ce,i}$ is an individual cylinder pressure without firing, $P_{comb,i}$ is the rise in cylinder pressure caused by combustion only and is the difference between P_i and $P_{ce,i}$.

In order to consider the torque only caused from combustion, it is defined as in the following equation by subtracting equation (10) from equation (7).

$$\bar{J}\ddot{\theta}_{syn,rev}=\bar{J}\ddot{\theta}_{syn}-\sum_{i=1}^{n}P_{ce,i}\frac{\partial V_i}{\partial\theta} \tag{11}$$

$\ddot{\theta}_{syn,rev}$ is the revised synthetic angular acceleration removed compression/expansion work from original synthetic angular acceleration.

If the nonlinear rotational dynamics is applied, the "synthetic" acceleration and speeds can be re-written.

$$\ddot{\theta}_{syn,rev}=\frac{J(\theta)}{\bar{J}}\ddot{\theta}+\frac{1}{2\bar{J}}\frac{\partial J(\theta)}{\partial\theta}\dot{\theta}^2-\frac{1}{\bar{J}}\sum_{i=1}^{n}P_{ce,i}\frac{\partial V_i}{\partial\theta} \tag{12}$$

$$\dot{\theta}_{syn,rev}=\frac{J(\theta)}{\bar{J}}\dot{\theta}-\frac{1}{2\bar{J}}\int\left(\frac{\partial J(\theta)}{\partial\theta}\dot{\theta}^2+2\sum_{i=1}^{n}P_{ce,i}\frac{\partial V_i}{\partial\theta}\right)dt \tag{13}$$

$P_{ce,i}$ can be measured for the target engine or calculated from an assumed polytropic process of compression and expansion between the intake port closing and the exhaust port opening.

$$P_{ce,i}=P_{ic}\left[\left(\frac{V_i(\theta_{ic})}{V_i(\theta)}\right)^k-1\right] \tag{14}$$

$$V_i(\theta)=\frac{\pi B^2}{4}\left[\frac{2R}{\varepsilon-1}+L+R(1-\cos\theta)-\sqrt{L^2-R^2\sin^2\theta}\right] \tag{15}$$

$$\frac{\partial V_i(\theta)}{\partial\theta}=\frac{\pi B^2}{4}R\sin\theta\left[1+\frac{R\cos\theta}{\sqrt{L^2-R^2\sin^2\theta}}\right] \tag{16}$$

3.2. Simulations

In order to check the influence of derived synthetic variables, simulations were conducted for an 1.4 liter, inline 4 cylinders gasoline Engine++ model, with the intention of verifying the differences between existence and nonexistence of misfires

3.2.1. Polar moment of inertia

Figures 3 and 4 show the variation of polar moment of inertia and its derivative with respect to crankangle. The moment of inertia is repeated periodically, and peaks occur near 90°, 270°, 450°, and 630° from the top dead center for cylinder 1 of the engine.

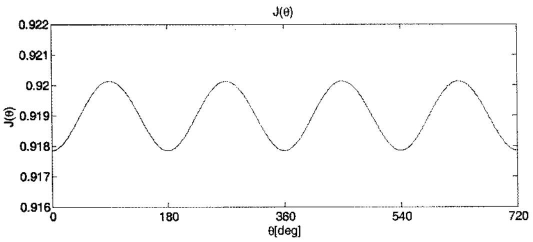

Figure 3. Variation of moment of inertia.

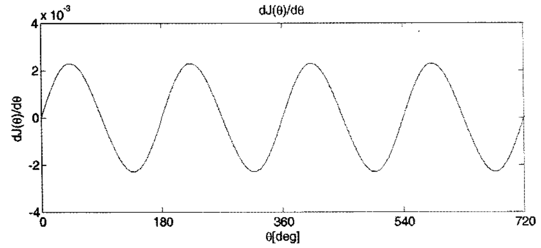

Figure 4. Derivative of moment of inertia.

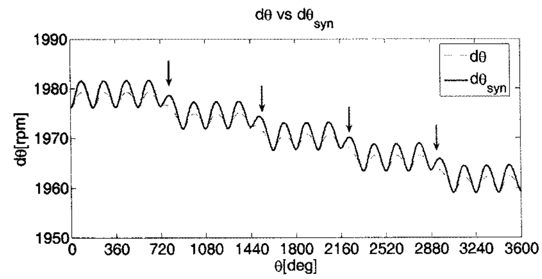

Figure 5. Speed and syn. speed around 2000 rpm.

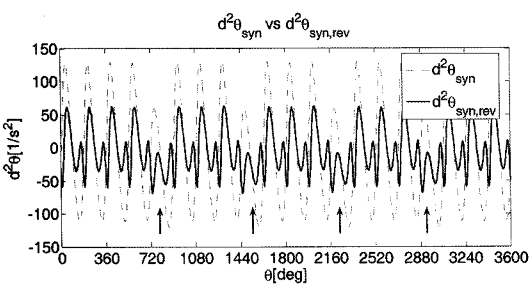

Figure 6. Syn. acceleration and revised syn. Acceleration.

3.2.2. Synthetic angular velocity

Figure 5 is a plot of the synthetic speed around 2000 rpm. There are four misfires around 720°, 1440°, 2160°, and 2880° which are indicated with the arrows

The dotted line represents the crankshaft angular speed, and solid line does synthetic speed. The peak-to-peak magnitude of synthetic speed is larger than that of crankshaft angular speed because synthetic speed is calculated by removing inertia effects from the angular speed.

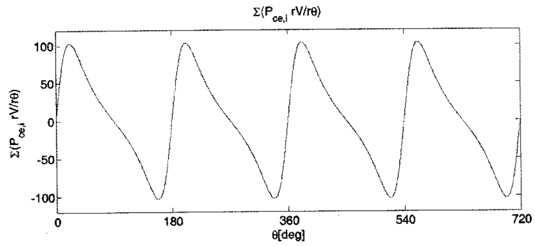

Figure 7. Compression and expansion work.

3.2.3. Revised synthetic angular acceleration

Figure 6 shows the revised synthetic angular acceleration by subtracting the compression/expansion work expressed by a waveform of Figure 7 from $\ddot{\theta}_{syn}$. It helps detecting misfire events easily since the pure torque generated by combustion can be obtained.

4. MISFIRE DETECTION

In this chapter, the misfire detection process using the neural network is described in terms of detection algorithm development and algorithm verification using simulation.

4.1. Detection Algorithm

There are several learning rules such as Hebbian, Widrow-Hoff, Kohonen, and Backpropagation which are generally used in learning neural networks. In this paper, the Backpropagation method is adopted because it is best for classifying patterns (Hagan *et al.*, 1995; Nigrin *et al.*,

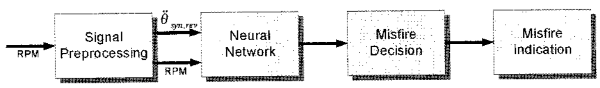

Figure 8. Schematic diagram of misfire detection system.

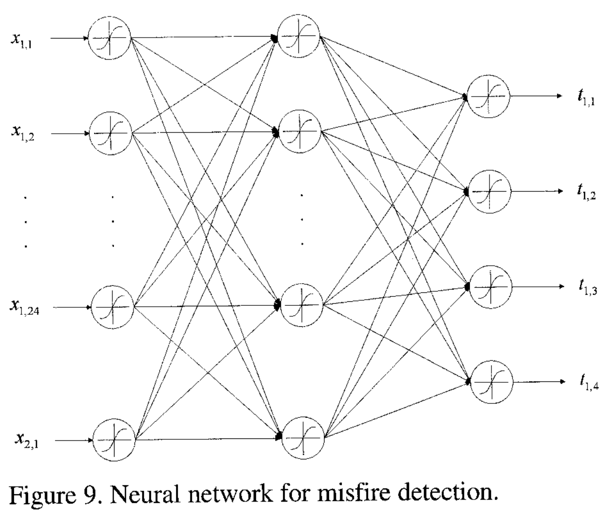

Figure 9. Neural network for misfire detection.

Table 1. Misfire detection rates of simulation for 4-cylinder engine. (unit %)

Speed	Misfire Pattern					
	Continuous Misfire				Random Misfire	No Misfire
	1	3	1, 3	2,4		
1000 rpm	100	99.8	99.6	99.4	99.2	99.8
2000 rpm	100	100	99.8	100	100	100
3000 rpm	99.8	100	99.6	99.8	99.6	100
4000 rpm	99.6	99.8	99.2	99.4	98.8	99.8

1993; Park *et al.*, 2001).

The procedure used in the misfire detection system is depicted in Figure 8. From the crankshaft encoder signal the angular velocity is calculated at 30° intervals. In the signal preprocessing stage, the revised synthetic angular acceleration is obtained. Then, and are applied to the neural network. At last, a misfire is determined by comparing the outputs of the neural network with a threshold value. A constructed neural network for detecting misfire is shown in Figure 9. The network is composed of three layers: the input, hidden, and output layer. The input layer has vectors of and which have sizes of 24 and 1 respectively. The hidden layer is composed of 12 neurons. The outputs are defined by a vector which indicates the portion of the misfire. The tansig function is used for the transfer function of each layer. The output values larger than 0.7 indicate that misfire occurs in the corresponding cylinder.

The neural network must be trained for detecting misfire events. The backpropagation rule is used for training, and this is the most important part of constructing the neural network. Since the network is trained using the input and output relationship of the system, the input and output data must be acquired for various engine operating conditions and misfire patterns.

The training is accomplished by determining the weight factors with the acquired data.

4.2. Verification of Algorithm

The simulink engine model is used for testing the neural network.

After calculating using the angular velocity acquired from the simulation results, the data are applied to the neural network. Because training has to be preceded in the misfire detection process, random and continuous misfire for single and multiple cylinder data are acquired at operation of 1000, 2000, 3000, and 4000 rpm under the various load conditions. About 500 cycles of data are captured under each condition creating a total acquired data set of approximately 20000 cycles. These data are used for training the neural network. The trained network is cross-validated using another simulation data set under the conditions referenced in Table 1. Table 1 shows that the total detection rate is as high as 99% for 5000 cycles (200 cycles 25 conditions).

5. EXPERIMENTAL RESULTS

The misfire detection system is validated by simulation in previous chapter. The combustion quality is varying for every cycle and there exist a noise which disturbs detecting misfire events. Because these are not appeared in simulation the misfire detection system must be verified with experimental results.

5.1. Experimental Environment

In this study, a 2-liter, inline-4-cylinder, CRDI diesel engine mounted on an EC dynamometer is used. The target signal is extracted from the pre-installed magnetic pickup sensor. A Micro-Autobox by dSPACE is utilized for operating engine.

5.2. Misfire Detection System Verification

5.2.1. Neural network training

Pattern recognition using neural network relies on the experience of the patterns, thus the neural network needs to be trained for the overall operating conditions. In order to obtain overall operating data, many experiments are conducted for the various conditions over 10000 cycles, focusing on the general engine operating points referenced in Table 2.

Table 2. Experimental conditions.

Items	Conditions
Engine speed	1000, 1500, 2000, 2500, 3000 rpm
Engine torque	3 kgfm~10 kgfm
Misfire	No misfire, Random misfire, Continuous misfire (Single & Multiple)

Table 3. Misfire detection rates for 4-cylinder engine with preprocessing. (unit %)

Speed	Misfire pattern			
	Continuous misfire		Random misfire	No misfire
	Single cyl.	Multiple cyl.		
1000 rpm	100	100	97.3	99.2
1500 rpm	98.3	97.5	99.2	99.8
2000 rpm	99.2	97.4	96.6	100
2500 rpm	99.5	98.3	94.8	98.2
3000 rpm	99.2	98.6	99.4	99.2

Table 4. Misfire detection rates for 4-cylinder engine without preprocessing. (uint %)

Speed	Misfire pattern			
	Continuous misfire		Random misfire	No misfire
	Single cyl.	Multiple cyl.		
1000 rpm	98.8	98.2	94.6	98.2
1500 rpm	97.7	95.7	98.7	98.7
2000 rpm	99.2	97.9	92.6	96.4
2500 rpm	97.9	96.2	90.1	93.6
3000 rpm	97.4	95.8	97.2	97.6

5.2.2. Misfire detection results

The experimental results are shown in Tables 3 and 4. Table 3 shows the results of the proposed misfire detection system with preprocessing, and Table 4 shows the results of the misfire detection system without preprocessing. The disagreements of these results are definitely as the results shown in the tables. The average detection rates are about 98% and 96% with and without preprocessing.

6. CONCLUSIONS

In this paper, the misfire detection system with synthetic variable method for preprocessing of crankshaft angular speed and neural network for detection algorithm is introduced. The effects of varying inertia due to crankshaft rotation and compression/expansion work are removed by the synthetic variable method. Consequently, the angular speed variation from combustion is remained. This method has advantages of detecting misfire events because the work output of each cylinder can be estimated. In addition the nonlinear rotational dynamics can be modeled as linear by this technique, and the speed dependency between waveform of the synthetic variables and the mean engine speed is completely eliminated. Based on these preprocessing the misfire detection algorithm is developed using a neural network. Prior to the experiments, the applicability of developed misfire detection system is evaluated by means of mathematical engine model simulations. Typical crankshaft speed fluctuation based misfire detection system has difficulties for detecting individual cylinder misfire events. The developed misfire detection system, however, allows detecting individual cylinder misfire events with high accuracy. Then the misfire detection system is validated by experimental data. In order to evaluate the effectiveness of preprocessing method, the results of the detection system with and without preprocessing are compared. Since it is possible to estimate the generated torque from combustion with the preprocessing technique, cylinder pressure can be reconstructed through further research. Furthermore it is expected that precise engine control can be achieved by the reconstructed cylinder pressure.

ACKNOWLEDGEMENT–This research was supported by the Research & Development Division of Hyundai Motor Company & Kia Motor Corporation with assistance of Mr. Kisang Lee and Dr. Seugbum Park. Also Engine++ was supplied by SimuQuest. We are very grateful for this support.

REFERENCES

Ceccarani, M., Rebottini, C. and Bettini, R. (1998). Engine misfire monitoring for a V12 engine by exhaust pressure analysis. *SAE Paper No.* 980518.

Főrster, J., Lohmann, A., Mezger, M. and Ries-Müller, K. (1990). Advanced engine misfire detection for SI-engines. *SAE Paper No.* 90855.

Hagan, M. T., Demuth, H. B. and Beale, M. (1995). Neural network design. *PWS Publishing Company.* Boston, MA. USA.

Mahieu, V., Duponcheele, P., Leduc, B., Vanhemelrijk, J. L., Morenville, M. and Dehout, P. (2000). Misfire detection on S. I. engines, by instantaneous torque analysis. *SAE Paper No.* 2000-01-0367.

Moskwa, J. J. and Wang, W. (2000). Simplified engine combustion diagnostics using "Synthetic" variables. *SAE Paper No.* 2000-01-0364.

Moro, D., Azzoni, P. and Minelli, G. (1998). Misfire pattern recognition in high performance SI 12 cylinder engine. *SAE Paper No.* 980521.

Nareid, J. and Lightowler, N. (2004). Detection of Engine Misfire events using an artificial neural network. *SAE Paper No.* 2004-01-1363.

Nigrin, A. (1993). *Neural Networks for Pattern Recognition.* Cambrige. MA. USA.

Park, S., Yoon, P. and Sunwoo, M. (2001). Cylinder pressure-based spark advance control for SI engines. *JSME Int. J.* Series B, **44, 2,** 305–312.

Shiao, Y., Pan, C. H. and Moskwa, J. J. (1994). Advanced dynamic SI engine modeling for diagnostics and control. *Int. J. Vehicle Design*, **15, 6,** 578–596.

VanDyne, E. A., Burckmyer, C. L. and Wahl, A. M. (2000) Misfire detection from ionization feedback utilizing the smartfire® plasma ignition technology. *SAE Paper No.* 2000-01-1377.

Villarino, R. and Böhme, J. F. (2004). Misfire Detection in Automotive engines using structure-borne sound. *SAE Paper No.* 2004-01-0520.

Willimowski, M. and Isermann, R. (2000). A time domain based diagnostic system for misfire detection in spark-ignition engines by exhaust-gas pressure analysis. *SAE Paper No.* 2000-01-0366.

Wu, Z. J. and Lee, A. (1998). Misfire detection using a dynamic neural network with output feedback. *SAE*

Paper No. 980515.

Yoon, M., Lee, W. and Sunwoo, M. (2005). Development and implementation of distributed hardware-in-the-loop simulator for automotive engine control systems. *Int. J. Automotive Technology* **6, 2,** 107–117.